

This item is the archived peer-reviewed author-version of:

Electrochemical reduction of CO_2 : effect of convective CO_2 supply in gas diffusion electrodes

Reference:

Duarte Miguel, De Mot Bert, Hereijgers Jonas, Breugelmans Tom.- Electrochemical reduction of CO_2 : effect of convective CO_2 supply in gas diffusion electrodes
ChemElectroChem - ISSN 2196-0216 - 6:22(2019), p. 5596-5602
Full text (Publisher's DOI): <https://doi.org/10.1002/CELC.201901454>
To cite this reference: <https://hdl.handle.net/10067/1639950151162165141>

Electrochemical reduction of CO₂: Effect of convective CO₂ supply in gas diffusion electrodes

Miguel Duarte^[1], Bert De Mot^[1], Jonas Hereijgers^[1], Tom Breugelmans^{*[1, 2]}

Abstract: The electrochemical reduction of carbon dioxide (CO₂) is a promising technology in the light of the energy transition and industrial electrification. In this study two different electrolyzer configurations, flow-through and flow-by mode, were analyzed for the production of carbon monoxide to resolve the CO₂ mass transfer limitation problem at high current densities in gas diffusion electrodes. These two configurations respectively state convective and diffusive flow inside the gas diffusion layer and their effect was studied on the cathodic performance of the electrolyzer for varying operating conditions: cathodic potential, electrocatalyst loading and Nafion content. In flow-through configuration a current density of 220 mA/cm² could be achieved at a Faradaic efficiency of 90%, whereas in flow-by configuration the current density was at the same Faradaic efficiency limited to 140 mA/cm². However, flow-through configuration has a few limitations, such as the lower energy efficiency due to the higher ohmic drop and the faster deactivation caused by crystallization of electrolyte salts inside the gas diffusion electrode. Therefore, flow-by is currently the most adequate configuration for long-term operation of electrolyzers for the reduction of CO₂ to CO. This study represents an essential step toward the application of electrolyzers for the electroreduction of CO₂.

Abbreviations

FE_{CO} – CO Faradaic efficiency;
 FB – Flow-by;
 FT – Flow-through;
 GDE – Gas diffusion electrode;
 J_{CO} – Partial current density towards CO;

Introduction

The rise in atmospheric greenhouse gas concentration has been linked to a global warming of 1.0 ± 0.2 °C since pre-industrial times ^[1]. The need for negative emissions to prevent a global warming superior to 1.5 °C has increased the attractiveness of carbon dioxide (CO₂) capture and utilization technologies. In this regard, the electrochemical conversion of CO₂ stands out for its ability to reduce CO₂ into value-added carbon-based products making use of electrical energy. In particular carbon monoxide (CO) is an interesting product in terms of revenue per mole of electrons since its production takes up only two moles of electrons per mole of CO₂ reduced ^[2]. Moreover, CO has broad applications in the chemical industry. The most significant one is its use in syngas in the Fischer-Tropsch process for the synthesis of multi-carbon compounds. The estimated annual production of CO is 18 million tonnes ^[3], mostly by means of steam reforming of natural gas and coal.

However, regarding an industrial implementation of electrochemical CO₂ electrolyzers towards CO there are still several challenges that must be solved. For electrolyzers to be commercially applicable, long-term stability and selectivity with current densities above 200 mA/cm² are required ^[4]. Consequently, the academic community has given much attention to improve the electrocatalyst. Today electrocatalysts exist that are active and selective enough to attain this current density of 200 mA/cm² when converting CO₂ to CO ^[5–7]. However, at these commercially relevant current densities, important aspects of the reaction environment are often overlooked, such as CO₂ depletion ^[8]. As a result catalytic activity is limited, hindering the CO₂ electrochemical reduction reaction performance ^[6,8–10]. Hence, efficient CO₂ supply towards the catalyst surface is of utmost importance to make electrochemical CO₂ electrolyzers industrially feasible.

Concerning the CO₂ flow configuration, electrolyzers can be divided into two classifications: flow-by (FB) and flow-through (FT) (Figure 1). In the flow-by configuration, CO₂ flows alongside the gas diffusion electrode (GDE) and only by diffusion enters the pores of the GDE. At the catalyst surface the CO₂ is adsorbed and reduced, followed by a desorption and diffusion step. As CO₂ in the flow-by configuration only enters the pores of the GDE through diffusion, a concentration gradient exists in the vicinity of the catalyst surface. Hence, severe effects of CO₂ depletion could occur in the FB configuration, hindering the electrode's performance. Moreover, catholyte that flows at the opposite side of the GDE can flood the GDE, typically due to electrowetting, blocking CO₂ diffusion paths which increases the concentration gradient even more ^[11]. This electrolyte flux is, however, crucial to avoid crystallization inside the pores of the carbon paper ^[9]. Therefore, the differential pressure across the GDE is a factor to take into account in the optimization of the cathodic performance as we thoroughly analyzed in previous work ^[12]. In the flow-through configuration the CO₂ is forced to flow through the GDE pores, diminishing the concentration gradient through the increased supply rate of CO₂ towards the catalyst surface. However, in the FT configuration gas bubbles emerge in the catholyte, increasing the ohmic drop ^[13]. Furthermore, in this configuration perspiration (i.e. small leakage of catholyte through the GDE towards the gas channel) can lead to electrolyte salt precipitation inside the GDE, blocking the GDE over time ^[9].

- [1] M. Duarte, B. De Mot, Dr. J. Hereijgers, Prof. Dr. T. Breugelmans
 Applied Electrochemistry & Catalysis (ELCAT)
 University of Antwerp
 Universiteitsplein 1, 2610 Wilrijk, Belgium
 E-Mail: Tom.Breugelmans@uantwerpen.be
- [2] Prof. Dr. T. Breugelmans
 Separation & Conversion Technologies, VITO
 Boeretang 200, 2400 Mol, Belgium.

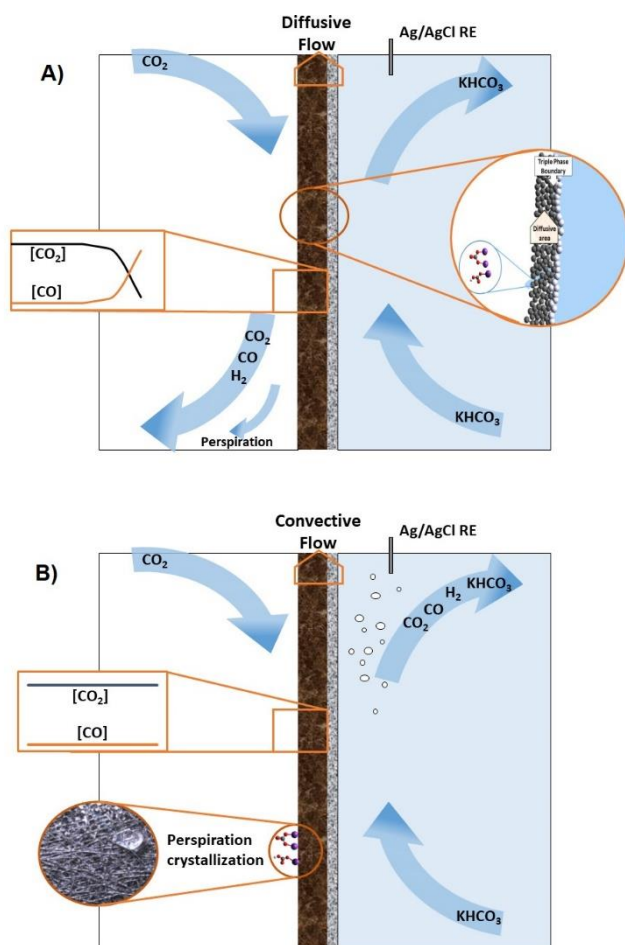
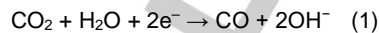


Figure 1. Flow configurations diagram: (A) Flow-by; (B) Flow-through.

Different membrane types have been reported in literature as suitable membrane for the electrochemical reduction of CO_2 , such as cation exchange membranes (CEM), generally Nafion,^[5,14–17] anion exchange membranes^[17–19], bipolar membranes^[20,21] and diaphragms^[6]. Nafion, is a thoroughly studied stable membrane with high ionic conductivity. In this application it has the purpose of upholding a neutral charge balance while preventing product cross-over from the catholyte to the anolyte. On the contrary anion exchange membranes do not prevent crossover of bicarbonate and formate ions to the anolyte^[22]. Bipolar membranes are, in its turn, unstable due to the formation of CO_2 in between the acidic and alkaline side causing delamination^[21]. However, Nafion is not only permeable to protons but also to cations like potassium that can migrate from the anolyte to the catholyte. Consequently, in the absence of catholyte (e.g. zero gap configuration) crystallization of potassium salts quickly occurs, deactivating the catalyst. Moreover, as the Nafion surface is acidic, the hydrogen evolution reaction is promoted. Consequently, catholyte between the GDE and membrane is needed to prevent a too acidic environment at the catalyst surface^[23]. On the other hand, if the catholyte is alkaline, the electrochemical reduction of CO_2 is compromised by the absorption of CO_2 to bicarbonate and carbonate, although alkaline media has been reported by *Dinh et al* to be beneficial for the cathodic overpotential of the cell^[5]. Even at a neutral pH it is not entirely possible to overcome this problem

due to basification of the local cathodic pH (≈ 12 at high current densities). This basification is due to the hydroxide formation as byproduct of the CO production (Eq. 1). Therefore, a neutralization reaction will occur in the presence of hydroxide ions and CO_2 . (Eq. 2). Consequently, it is of utmost importance to replenish the catholyte to keep this basification effect to a minimum.



While abundant research has focused on the catalyst and support development^[24–28], a thorough analysis between the two different CO_2 electrolyzer configurations (flow-by and flow-through) is still lacking^[3]. Is the increased CO_2 supply in flow-through worth the higher ohmic resistance caused by CO_2 bubbles in the electrolyte? Or is it advantageous to operate the cell in flow-by in order to optimize the electrolyzer energy efficiency? Moreover, for each reactor configuration it is expectable that the optimal gas diffusion electrode characteristics are different. A systematic approach for the study of FB and FT is necessary to avoid research operation under unreasonable conditions, both in electrochemical and economic viability terms. Here for the first time this analysis is being made using the same reactor and operating conditions, allowing an in-depth comparison of both configurations.

Materials and methods

An ElectroCell Micro Flow Cell® was adapted to guarantee membrane and GDE structural support and to allow the insertion of a leak free Ag/AgCl reference electrode (Innovative Instruments, Inc.) in the catholyte 1 mm away from the cathode (Figure 2). To this end, Viton gaskets and PMMA spacers were fabricated in-house using a CNC mill (Euromod MP45, Imes). Insertion of the reference electrode allowed the control of the cathodic potential independently of the anode. The electrolyzer was operated in a vertical position at room temperature and atmospheric pressure.

As cathode a 10.2 cm^2 Sigracet® 39 BC carbon paper was used as gas diffusion electrode. These carbon papers were coated with silver electrocatalytic nanoparticles by airbrushing. To this end, inks were prepared with silver powder ($< 100 \text{ nm}$, 99.5%, Sigma-Aldrich), 5% Nafion perfluorinated resin solution (Sigma-Aldrich), isopropanol (VWR) and ultrapure water (Milli-Q gradient, Millipore). After mixing and sonicating, the inks were airbrushed (Airbrush Gun AB-200) onto the carbon paper using argon as carrier gas. During this airbrushing, the substrate was placed on a hotplate at 100°C to guarantee sufficiently fast solvent evaporation and catalyst layer uniformity. The carbon paper was weighed before and after spraying to accurately determine the electrocatalyst loadings. As electrocatalyst sub 100 nm silver nanoparticles were used as it was reported that the onset potential for the production of CO was minimized at these particle sizes^[29]. Nafion 117 (Fuel Cell Store) was used as cation exchange membrane. A pre-treatment of the membrane was performed, which consisted of boiling the membrane first in H_2O_2 3%, subsequently in distilled water, then in 1M H_2SO_4 and finally in distilled water again, for 1 hour each time. Its purpose was on one hand to clean the membrane of organic contaminants and on the other to increase its water content, increasing also its ionic conductivity^[30]. Experiments were always preceded with half an hour of operation at open circuit potential in order to avoid effects of the shrinking of the membrane when changed to the potassium ionic form.

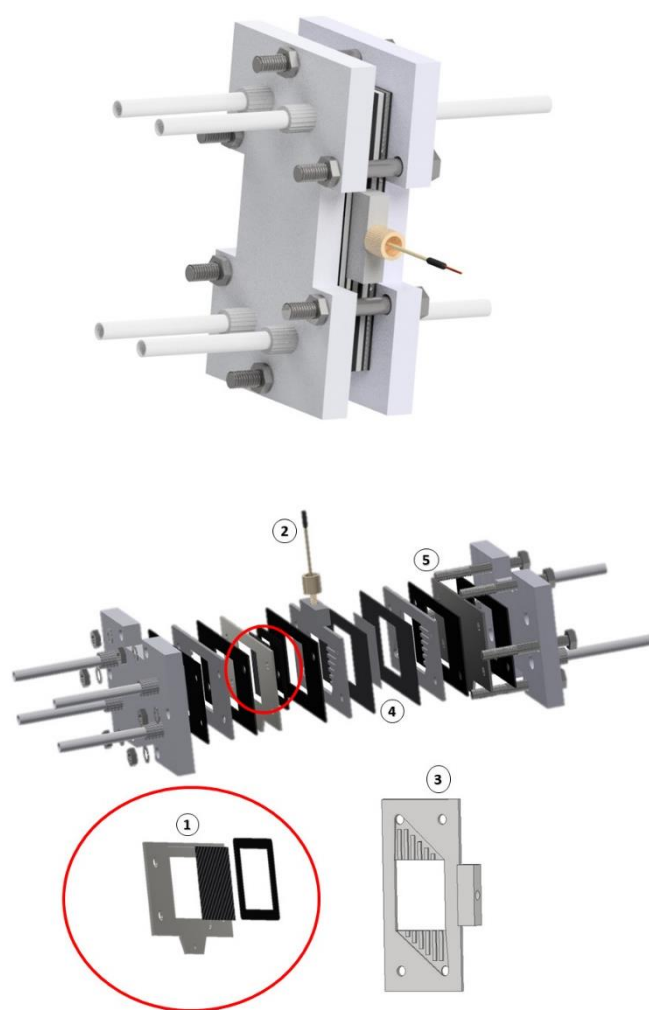


Figure 2. Scheme of the reactor: 1) Cathode: Titanium frame, Gas diffusion electrode, Gasket for GDE preservation; 2) Ag/AgCl leak-free reference electrode; 3) Catholyte spacer built for better Nafion support and compatibility with RE; 4) Nafion CEM; 5) Platinized titanium anode.

CO₂ was purchased from Nippon, and its flow rate was controlled with a Brooks Instrument GF-40 mass flow controller to 77 mL/min (7.55 mL CO₂/min·cm²). Before entering the reactor, CO₂ was humidified by sparging it in water. The anolyte consisted of 0.5L 2M KOH (VWR, assay 85%) and the catholyte of 0.5L 2M KHCO₃ (Acros Organics, >99.5%). Both the anolyte and catholyte were recirculated with a flow rate of 10 mL/min and 15 mL/min respectively. The anolyte was pumped with an Ismatec Reglo ICC peristaltic pump and the catholyte was pumped with an HPLC pump (Watrex DeltaChrom P102). A Swagelok ball valve was inserted at the reactor's gas outlet for alternation between flow configurations (FB and FT). The potential was controlled with a multichannel Autolab potentiostat M204 equipped with an FRA module and a 10A booster. In flow-through, the gas bubbles between the GDE and the reference electrode were responsible for an additional ohmic drop. Consequently, for reactor configuration comparison, active IR compensation was

implemented. Electrochemical impedance spectroscopy (EIS) measurements were performed before every experiment in order to accurately measure the extra resistance. Bode plots were analyzed and the ohmic resistance was measured at a frequency of 10 kHz. The additional resistance between the cathode and the reference electrode caused by gaseous flow in the catholyte chamber in the flow-through configuration accounted on average to 0.1 ohm.

The gas samples were analyzed with an in-line Shimadzu 2014 series gas chromatograph equipped with a TCD detector and a micropacked column (Restek Shincarbon ST, 2 m length, 1 mm internal diameter, 100/120 mesh). The initial oven temperature was set at 40 °C. After maintaining it for 3 minutes it was ramped up to 250 °C at 40 °C/min, at which point it was sustained for 3 minutes. The TCD detector was kept at 280 °C and helium was used as carrier gas at a flow rate of 10 mL/min. The gas stream was separated from the liquid phase in an in-house built gas/liquid separator and subsequently filtered with an in-house built glass fiber filter, to trap any residual liquid droplets. The values reported below for the Faradaic efficiency and partial current density for CO were averaged for 3 measurements. Likewise, the error analysis data presented is based on the standard deviation of these 3 measurements.

Results and Discussion

Potential screening

To assess the influence of the applied potential on the catalyst selectivity and activity, a series of experiments of 2.5 hours at different cathodic potentials were performed for both flow configurations. A fresh GDE with a 0.75 mg/cm² silver loading and 9% Nafion content was used for every experiment to exclude any stability influences. Only CO and H₂ were formed at a significant rate. By HPLC analysis formic acid was detected, but only accounted to less than 1% Faradaic efficiency.

In Figure 3 it can be observed that the flow-by configuration showed to be more selective towards CO at potentials more positive than -1.8V vs. Ag/AgCl. At -1.6 and -1.8 V vs Ag/AgCl the FE_{CO} was respectively 22% and 14% larger in the flow-by configuration than in the flow-through configuration. At more negative cathodic potentials than -1.8 V vs Ag/AgCl a difference in FE_{CO} trend stopped being clear. However, at these cathodic potentials the flow- through configuration achieved far greater current densities for CO (61% higher at -2.4 V vs Ag/AgCl and 77% at -2.8 V vs Ag/AgCl). This difference is most-likely due to a more efficient mass transfer where on the other hand it limits the partial current density to around 120 mA/cm² in FB configuration. At -2.2 V the current density reached a plateau in FB configuration as transport resistance became the limiting factor, impeding a further increase of the current density. At this plateau at -2.2 V vs. Ag/AgCl the yield towards CO was 0.91 mL/cm²·min⁻¹ for the FB configuration. The flow-through configuration allowed to overcome the 200 mA/cm² threshold, by providing an excess CO₂ environment and achieved a yield towards CO of 1.45 mL/cm²·min.

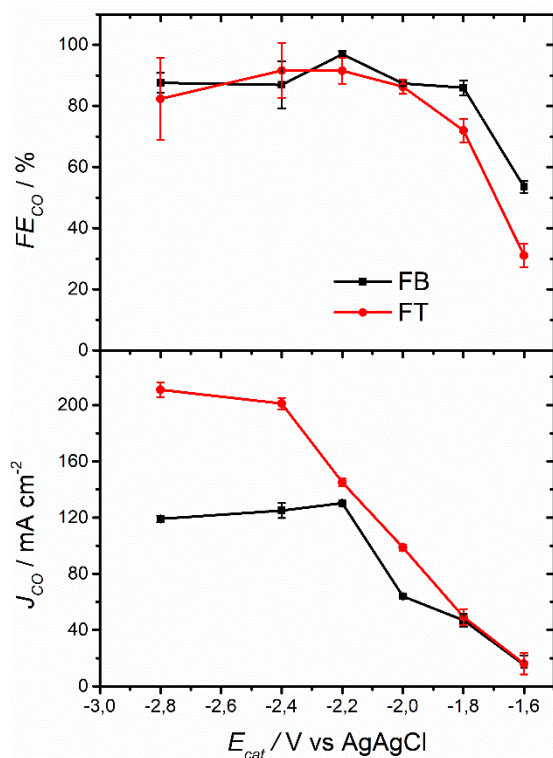


Figure 3. Influence of the cathodic potential on the (A) selectivity and (B) partial current density for CO with GDEs loaded with 0.75 mg Ag/cm² and 9% Nafion content.

While FB and FT had a comparable performance at low overpotentials, the FT was clearly more advantageous for the mass transfer limited region. In a CO₂ deficit environment, the proton competition for the active sites became relevant, hindering the performance of the CO₂ reduction and favoring the hydrogen evolution reaction^[8]. Accordingly, the current density for CO reached a plateau at the rate of the diffusive supply of CO₂ to the active sites governed by the concentration gradient developed through the gas diffusion layer.

Catalyst loading influence

From the previous results (Figure 3) it was clear that at -2.0 V vs Ag/AgCl neither of the configurations was operating in the mass transfer limited region. Furthermore, both configurations achieved already at this potential high Faradaic efficiencies towards CO (92% in FB; 86% in FT). This implies that CO₂ at the catalyst was not depleted and that higher CO production rates can be obtained with higher catalyst loadings. To this end, the catalyst loading was varied for the FT and FB configuration and the FE_{CO} and the current density determined at a cathodic potential of -2.0 V vs Ag/AgCl. From Figure 4 B it was clear that the FT configuration succeeded in increasing the current density at the same FE_{CO} . Consequently, the CO production rate could be increased, merely by increasing the catalyst loading, indicating that the factor which was limiting was the availability of reaction sites. However, the increase in activity was not proportional to the increase in catalyst mass, since the mass based partial current density for CO decreases up until a catalyst loading of 1.25 mg/cm² (Figure 4 C).

The FB configuration due to mass transfer limitation did not show a higher production rate with higher catalyst loading. The unavailability of CO₂ showed once more to be the main weakness in the flow-by configuration, being the turnover frequency limited by the rate of CO₂ and CO/ H₂ diffusion.

At a high catalyst loading of 2.0 mg/cm² the current density and selectivity in FB did increase. Actually, an analysis of the electrode's activity in relation to the mass of catalyst sprayed shows the advantage of working at high catalyst loadings since at high catalyst loading the mass based current density stabilized and the geometric partial current density was maximal. Examining the partial current densities per milligram of catalyst at high loadings in FB and FT, no reduction can be seen between 1.25 mg/cm² and 2 mg/cm², being discernible even a slight increase in performance in FT. Hence, even in flow-by, due to the increased active area a more efficient CO₂ conversion was achieved. Operation without silver nanoparticles, as expected, showed virtually no selectivity towards CO (< 0.3%).

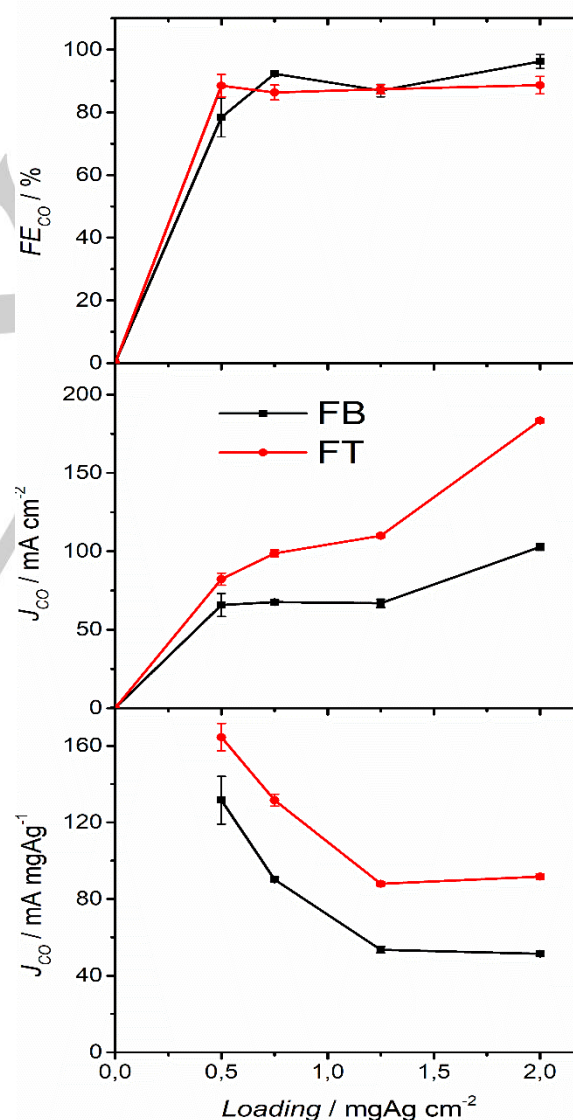


Figure 4. Influence of the silver nanoparticles loading on the (A) selectivity, (B) geometric partial current density and (C) mass based partial current density for CO at $E_{cat} = -2$ V vs Ag/AgCl and 9% Nafion content GDEs.

Nafion ionomer loading

The incorporation of Nafion ionomer in the catalyst ink is known for having an effect on its stability due to the creation of an additional repulsive interaction between the particles in the form of steric interaction^[31]. Furthermore, an optimal loading of Nafion leads to the formation of a continuous frame network that allows ionic conductivity while maintaining electrical conductivity^[32,33]. The ionomeric binder content also influences the availability of active sites due to on one hand extending the active surface area and on the other blocking catalyst nanoparticles. Additionally, the hydrophilicity of Nafion ionomer changes the wettability of the GDE controlling the amount of perspiration and the diffusion of the CO₂^[34]. To this end, the Nafion ionomer loading was varied from 3% (w/w) to 40% (w/w). At 3% (w/w) of Nafion ionomer loading, the bonding strength of the nanoparticles to the carbon paper was not strong enough. Detachment of catalyst nanoparticles from the GDE surface was clearly visible due to the coloration of the electrolyte.

This effect was more pronounced in the FT configuration as can also be seen by its selectivity drop (Figure 5). In the FT configuration the shear forces were much larger as CO₂ was forced through the GDE. Between 9% and 20% (w/w) Nafion ionomer loading no difference in selectivity and current density was observed for the same flow configuration.

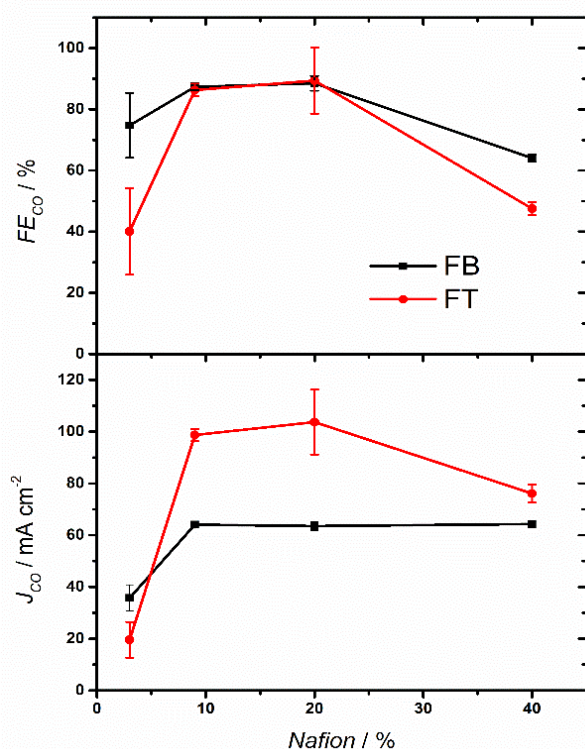


Figure 5. Influence of the Nafion/catalyst percentage (w/w) of the GDE on the (A) selectivity and (B) partial current density at $E_{\text{cat}} = -2$ V vs Ag/AgCl and a loading of 0.75 mg Ag/cm².

However, comparing the FT and FB configuration, FT showed a 40 mA/cm² larger current density than the FB configuration for 9% and 20% (w/w) Nafion loading. This enhancement is attributed to the same cause stated for the experiments with different cathodic potentials and catalyst loadings – a boosted CO₂ supply. By

increasing the Nafion ionomer loading up to 40% (w/w), the FE_{CO} drastically decreased in both configurations (28% for FB and 47% for FT). This selectivity may be related to the lower local pH caused by Nafion acidic properties which shifts the selectivity to the HER. However, the scarcity of protons in a 2 M KHCO₃ electrolyte point to the conclusion that the greater role here is played by the blockage of active sites by the ionomer. The results obtained were in agreement with recent studies which optimized the binder content to 11.1%^[35] and 20%^[36]. In this loading window, a balance between ionic conductivity, pH, hydrophilicity, electrical conductivity and active sites availability is achieved leading to optimal performance.

Stability

To assess the stability of the electrodes, long-term experiments of 10 hours were conducted to study the stability of the catalyst in both flow configurations at a cathodic potential of -2.0 V vs Ag/AgCl, a loading of 0.75 mg Ag/cm² and 20% Nafion content. The results presented in Figure 6 show a fast deactivation after one hour of operation in flow-through as a result of the crystallization of electrolyte salts inside the gas diffusion layer pores blocking the diffusion of CO₂ to the active sites. To assess if this deactivation was partially caused by catalyst detachment an ICP-MS analysis of the electrolyte sampled after 10 hours of operation was performed. The analysis revealed absence of silver in the electrolyte (detection limit of 0.5 ppm). The nanoparticles stability was supported by an analysis of the scanning electron

microscopy (SEM) pictures presented in Figure 7 A – C. The images B and C show a uniform catalyst layer in the end of long-term operation both in FB and FT. Moreover, there is no evident difference in catalyst cover between these and image A that displays a fresh GDE. In Figure 7 D it is clearly visible the crystallization associated with the GDE deactivation. After this deactivation, the performance of flow-through remained stable for 3 hours operating at a partial current density towards CO of

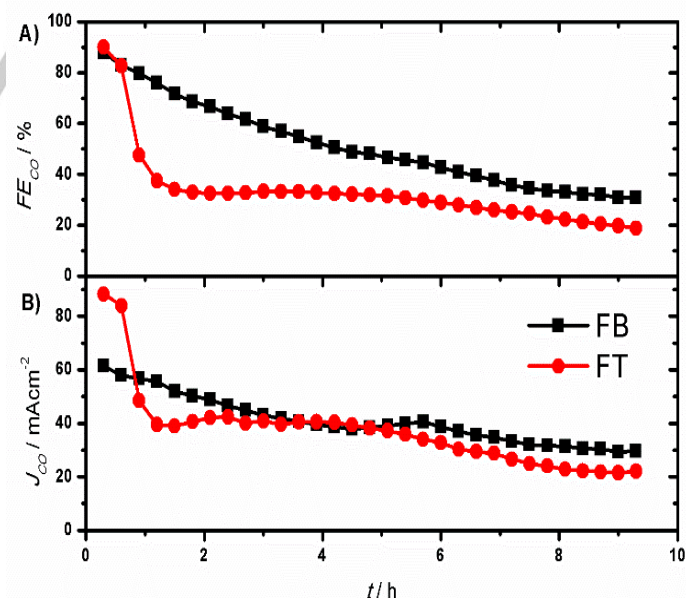


Figure 6. 10 hours experiments with 0.75 mg/cm² loading and 20% Nafion content in FB and FT at $E_{\text{cat}} = -2$ V vs Ag/AgCl: (A) Faradaic efficiency and (B) partial current density.

around 40 mA/cm², followed by a gradual slow decrease until the end of the experiment. In flow-by configuration, the cathodic activity was inferior during the first hour, but its stability was superior to flow-through although performing also gradual and slowly worse towards the end of the experiment. This deactivation is also a consequence of the perspiration rate that gradually hinders the CO₂ diffusion. It is important to point out the similarity in the failure mechanisms that lead to a selectivity drop which is in both configurations the blockage of active sites by either electrolyte that floods the carbon paper or its crystallization inside the pores of the carbon paper. The deactivation profile is expected to be the same for operation at different cathodic potential, since this is independent of the failure mechanism, whereas the decrease in activity and selectivity is expected to proceed for longer times as crystallization effects will become more severe over time.

Energy efficiency

Finally, the biggest limitation of flow-through configuration is the lower energy efficiency caused by the gas bubbles forced through the gas diffusion electrode into the catholyte. This additional resistance results in an increase of 1.0 V in cell potential and an energy efficiency (Equation 3) drop of around 6.5 % in comparison with flow-by.

$$\varepsilon_{\text{energy}} = \frac{(E_{\text{CO}}^0 + E_{\text{O}_2}^0) \cdot FE_{\text{CO}}}{E_{\text{cell}}} \quad (3)$$

As mentioned in Materials and methods, a difference of 0.10 ohm was measured between FB and FT when comparing the ohmic resistance between the cathode and the reference electrode. However, when taking the total resistance between cathode and anode into account, there is a difference of 0.18 ohm between both configurations (Table 1). This is due to the CO₂ and products bubbles between the reference electrode and the Nafion membrane.

Table 1. Energy efficiency data during operation at $E_{\text{cat}} = -2$ V vs Ag/AgCl, 0.75 mg Ag/cm², 9% Nafion.

	Flow-by	Flow-through
Energy efficiency (%)	32.5	26
Faradaic efficiency (%)	86.3	87.4
Cell potential (V)	3.9	4.9
Cell resistance (Ω)	1.07	1.25

Being the electricity supply the main operating cost of the technology [37], it is imperative that the energy efficiency is optimized. Further research should be undertaken to overcome the stability issues of flow-through reactor configuration and minimize its ohmic drop. The use of lower molarity electrolytes may slow down crystallization inside the GDE. Likewise, optimization of the CO₂ flow may also play an important role in stability, avoiding adverse preferential flows and electrolyte crystallization.

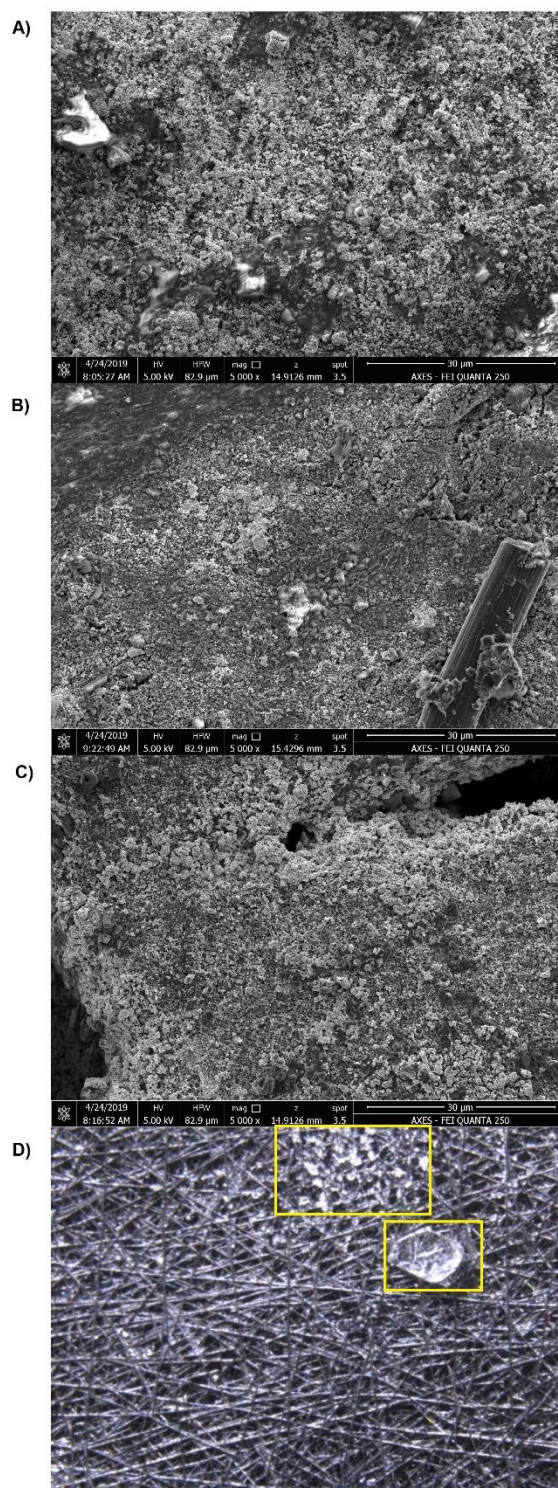


Figure 7. SEM picture of (A) fresh GDE, (B) GDE after 10 hours of operation in flow-by configuration, (C) GDE after 10 hours of operation in flow-through configuration; (D) optical microscopy picture of crystallization on the back of the GDE after flow-through operation.

Conclusions

The implementation of convective flow inside the gas diffusion layer was for the first time scrutinized in comparison with a diffusive flow-by configuration. Remarkably, both flow configurations achieved high Faradaic efficiencies towards CO (>90%) at moderate overpotentials. FT seemed to stand out especially when operating with higher loadings and at higher overpotentials due to the enhanced CO₂ supply to the catalyst surface. However, the lower energy efficiency caused by a higher ohmic drop compromises its viability. Furthermore, electrolyte crystallization in the GDE pores severely limits the catalyst selectivity for long-term operation. Hence, FB outperforms FT and remains the most efficient configuration for long-term operation of electrolyzers for the reduction of CO₂ to CO. The insights gained from this work add to the growing number of reports of high current density towards CO, reporting the optimal working conditions for both reactor configurations. The pivotal role of operating on a CO₂ excess environment was established and the findings of the research strengthen the idea that the development of more stable gas diffusion electrodes and CO₂ supply optimization is a promising field to achieve higher current densities and develop commercially viable CO₂ electrolyzers for the production of CO.

Acknowledgements

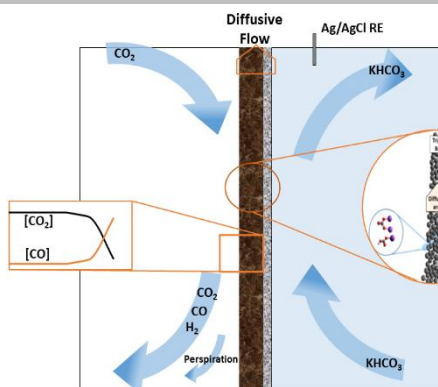
B. De Mot was supported through a PhD fellowship of the Industrial Research Fund – Flanders (IOF). J. Hereijgers was supported through a postdoctoral fellowship (28761) of the Research Foundation – Flanders (FWO). This project was funded by the Interreg 2 Seas-Program 2014-2020, cofinanced by the European Fund for Regional Development in the frame of subsidiary contract nr. 2S03-019.

Keywords: CO₂ utilization • Electrochemical reduction of CO₂ • Electrochemistry • Gas diffusion electrode • Sustainable chemistry

References

- [1] M. Allen, O. P. Dube, W. Solecki, F. Aragón-Durand, W. Cramer, S. Humphreys, M. Kainuma, J. Kala, N. Mahowald, Y. Mulugetta, *IPCC* **2018**, 32.
- [2] C. Chen, J. F. K. Kotyk, S. W. Sheehan, *Chem* **2018**, 4, 2571–2586.
- [3] B. Endrődi, G. Bencsik, F. Darvas, R. Jones, K. Rajeshwar, C. Janáky, *Prog. Energy Combust. Sci.* **2017**, 62, 133–154.
- [4] S. Verma, B. Kim, H. R. M. Jhong, S. Ma, P. J. A. Kenis, *ChemSusChem* **2016**, 9, 1972–1979.
- [5] C. T. Dinh, D. Sinton, *ACS Energy Lett.* **2018**, 3, 2835–2840.
- [6] T. Haas, R. Krause, R. Weber, M. Demler, G. Schmid, *Nat. Catal.* **2018**, 1, 32–39.
- [7] H. M. Jhong, S. Ma, P. J. A. Kenis, *Curr. Opin. Chem. Eng.* **2013**, 2, 191–199.
- [8] T. Burdyny, W. A. Smith, *Energy Environ. Sci.* **2019**, 12, 1442–1453.
- [9] P. Jeanty, C. Scherer, M. Erhard, K. Wiesner-Fleischera, O. Hinrichsenb, M. Fleischera, *J. CO₂ Util.* **2018**, 24, 454–462.
- [10] R. L. Cook, R. C. MacDuff, A. F. Sammells, *J. Electrochem. Soc.* **1990**, 137, 607.
- [11] T. Burchardt, *J. Power Sources* **2004**, 135, 192–197.
- [12] B. De Mot, J. Hereijgers, M. Duarte, T. Breugelmans, *Chem. Eng. J.* **2019**, 378, 122224.
- [13] J. Vennekoetter, R. Sengpiel, M. Wessling, *Chem. Eng. J.* **2019**, 364, 89–101.
- [14] E. Irtem, T. Andreu, A. Parra, M. D. Hernández-Alonso, S. García-Rodríguez, J. M. Riesco-García, G. Penelas-Pérez, J. R. Morante, *J. Mater. Chem. A* **2016**, 4, 13582–13588.
- [15] B. Kim, S. Ma, H. R. M. Jhong, P. J. A. Kenis, *Electrochim. Acta* **2015**, 166, 271–276.
- [16] E. J. Dufek, T. E. Lister, M. E. McIlwain, *J. Appl. Electrochem.* **2011**, 41, 623–631.
- [17] B. Endrődi, E. Kecsenovity, A. Samu, F. Darvas, R. V. Jones, V. Török, A. Danyi, C. Janáky, *ACS Energy Lett.* **2019**, 4, 1770–1777.
- [18] R. B. Kutz, Q. Chen, H. Yang, S. D. Sajjad, Z. Liu, I. R. Masel, *Energy Technol.* **2017**, 929–936.
- [19] K. P. Kuhl, E. R. Cave, D. N. Abram, T. F. Jaramillo, *Energy Environ. Sci.* **2012**, 5, 7050–7059.
- [20] A. Patru, T. Binninger, B. Pribyl, T. J. Schmidt, *J. Electrochem. Soc.* **2019**, 166, F34–F43.
- [21] Y. C. Li, Z. Yan, J. Hitt, R. Wycisk, P. N. Pintauro, T. E. Mallouk, *Adv. Sustain. Syst.* **2018**, 1700187, 1700187.
- [22] H. Yang, J. J. Kaczur, S. D. Sajjad, R. I. Masel, **2017**, 20, 208–217.
- [23] C. Delacourt, P. L. Ridgway, J. B. Kerr, J. Newman, *J. Electrochem. Soc.* **2008**, 42–49.
- [24] Y. Wu, J. Jiang, Z. Weng, M. Wang, Y. Zhong, G. W. Brudvig, Z. Feng, H. Wang, *ACS Cent. Sci.* **2017**, 3, 847–852.
- [25] M. Asadi, B. Kumar, A. Behranginia, B. A. Rosen, A. Baskin, N. Reprin, D. Pisasale, P. Phillips, W. Zhu, R. Haasch, et al., *Nat. Commun.* **2014**, 1–8.
- [26] Y. Zhao, C. Wang, G. G. Wallace, *J. Mater. Chem. A* **2016**, 4, 10710–10718.
- [27] S. Ma, Y. Lan, G. M. J. Perez, S. Moniri, *ChemSusChem* **2014**, 7, 866–874.
- [28] H. Mistry, A. S. Varela, C. S. Bonifacio, I. Zegkinoglou, I. Sinev, Y. W. Choi, K. Kisslinger, E. A. Stach, J. C. Yang, P. Strasser, et al., *Nat. Commun.* **2016**, 7, 1–8.
- [29] M. S. Jee, H. S. Jeon, C. Kim, H. Lee, J. H. Koh, J. Cho, B. K. Min, Y. J. Hwang, *Appl. Catal. B Environ.* **2016**, 180, 372–378.
- [30] R. Kuwertz, C. Kirstein, T. Turek, U. Kunz, *J. Memb. Sci.* **2016**, 500, 225–235.
- [31] S. Shukla, S. Bhattacharjee, A. Z. Weber, M. Secanell, *J. Electrochem. Soc.* **2017**, 164, F600–F609.
- [32] J. Wu, P. P. Sharma, B. H. Harris, X. D. Zhou, *J. Power Sources* **2014**, 258, 189–194.
- [33] E. Passalacqua, F. Lufrano, G. Squadrito, A. Patti, L. Giorgi, *Electrochim. Acta* **2001**, 46, 799–805.
- [34] O. G. Sánchez, Y. Y. Birdja, M. Bulut, J. Vaes, T. Breugelmans, D. Pant, *Curr. Opin. Green Sustain. Chem.* **2019**, 16, 47–56.
- [35] Q. Wang, H. Dong, H. Yu, H. Yu, *J. Power Sources* **2015**, 279, 1–5.
- [36] B. Kim, F. Hillman, M. Ariyoshi, S. Fujikawa, P. J. A. Kenis, *J. Power Sources* **2016**, 312, 192–198.
- [37] M. Jouny, W. W. Luc, F. Jiao, *Ind. Eng. Chem. Res.* **2018**, 57, 2165–2177.

Two different CO₂ electrolyzer configurations, flow-through and flow-by mode, were analyzed for the production of carbon monoxide to resolve the CO₂ mass transfer limitation problem at high current densities in gas diffusion electrodes. In flow-through configuration a current density of 220 mA/cm² could be achieved at a Faradaic efficiency of 90%, whereas in flow-by configuration the current density was at the same Faradaic efficiency limited to 140 mA/cm².



*M. Duarte, B. De Mot, J. Hereijgers, T. Breugelmans**

1 – 8

**Electrochemical reduction of CO₂:
Effect of convective CO₂ supply in
gas diffusion electrodes**